Vol.2 Issue.4, April 2014. Pgs: 38-52

IJRAME
ISSN (ONLINE): 2321-3051

INTERNATIONAL JOURNAL OF RESEARCH IN AERONAUTICAL AND MECHANICAL ENGINEERING

Damage Modeling in Reinforced Concrete Shelters Subjected to Ballistic Impact

Thiago B. N. de Melo[1], Mauricio V. Donadon[2]

[1] *Institute of Aeronautics and Space (IAE), braidotbnm@iae.cta.br*
[2] *Instituto Tecnologico de Aeronautica (ITA), donadon@ita.br*
Author Correspondence: Instituto Tecnológico de Aeronáutica ITA-CTA-IEA, São José dos Campos-SP, Brazil, +55-12- 39473613

Abstract

This work focuses on the development of a numerical model to predict the ballistic response of reinforced concrete shelters subjected to high velocity impact induced by penetration bombs, and the dynamic response of the case of the bomb. The dynamic response of reinforced concrete shelters was modelled using the Johnson-Holmquist JH2 model. The Johnson-Cook model combined with an equation of state (EOS) for explosives were used to model the transient dynamic response of the bomb. Three different bomb geometries were investigated in this work. A comparison in terms of ballistic impact resistance on the reinforced concrete shelter is presented and conclusions are drawn.

Keywords: High velocity impact, finite elements, composite materials, reinforced concrete.

1. Introduction

The concrete is a highly versatile constructive material, which can be cast into many shapes, and can be formulated for varying degrees of strength and durability. It is primarily used due its compressive strength, because concrete is much stronger in compression than it is in tension. With the proper use of tensile reinforcement, concrete can be used in many tensile loaded applications, such as flexural members, eccentrically loaded members, and even direct tension members (Cargile et al., 2002).

As published by Teng et al. (2004), Polanco – Loria et al. (2008) and Liu et al. (2011), the reinforced concrete has been used for a long time to construct military protective structures, like command and control centers, bunkers and shelters. Then, the penetrability of concrete structures when impacted by projectiles and the blast effects are of great interest for engineers to design the protective structures or weapon systems. Nowadays, it is still an open field for research.

The analysis of reinforce concrete target when impacted by projectiles is very complicated due the complex stress states acting on material, and the damage mechanism activated depends on the load path imposed (Polanco – Loria et al. ,2008). The principal overall responses of a reinforce concrete depends on the kinetic energy of the projectile and the strength characteristics of the reinforced concrete wall (Martin, 2010).

Empirical formulae on penetration depth, perforation thickness and scabbing thickness in a thick concrete target had been reviewed in 1976 by Kennedy (1976). In 2010, Rahman (2010) published a review of the new advances in empirical methods of penetration in concrete.

Full-size scale test is very expensive to make, and often the data is classified. Then, it is more usual to find small scale testing such as in the references (Hanchak (1992), DancYgier and Yahkelevsky (1996), Unusson and Nilsson (2006), Conrad (2011), Svinsas et al. (2001), Riedel et al. (1997)).

Several analytical studies on impact of projectiles have been reviewed by Gabi Ben – Dor et al. (2005) that presented review article including 280 references of analytical studies in plate penetration. Hughes (2004) presented an analytical study of the impact in reinforced concrete, and proposed a formula based on dimensional analysis. Chen et al. (2004) made an analytical study of non-deformable projectiles with different geometrical characteristics in metals, concrete and soil. Li et al. (2003) proposed analytical dimensional formulas to the penetration depth of rigid penetrators in concrete targets. Chen et al. (2004) presented an analytical study of normal and oblique penetration in concrete targets by rigid penetrators.

In recent years the numerical simulation of the penetration process has been advanced very far with the improvements of memory and speed of the computers. Several new constitutive models have been proposed to simulate the damage behaviour in the penetration processes (Liu, 2011). The use of numerical models has the advantage that is possible to estimate the stress and strains on the projectile, not only on target such in the analytical models. It is very useful to the development of new weapons.

Taylor et al. (1986), proposed a continuum damage model, called TCK for concrete penetration. Schwer and Day (1991) presented several computational techniques for impact simulation. Johnson and Holmquist (1992) presented a material model called JH1, which is used to predict the behaviour of fragile materials subjected to high strains, strain rates and pressures. In 1993 the model was improved by the same authors by including a damage variable that accounts for the continuum loss of the mechanical properties of the material with the increase of the damage variable. In 1993 Johnson, Holmquist and Cook (1993) developed the HJC model to describe the behaviour of the concrete when subjected to high strains, and using the confinement effects (hydrostatic pressure), strain rates and damage in the concrete strength. The HJC was used in several previous works related to impact in concrete (Liu et al. (2011), Conrad (2011), Tai and Tang (2006)). Polanco-Loria et al. (2008) modified the HJC to account the third invariant of the deviatoric stress and the strain rate sensitivity to improve the damage model. Liam et al. (2011) successfully used the HJC in a meshless code.

This work aims at investigating the influence of the ogive shape of penetration bombs on the penetrability of shelters. A shelter was simulated by a single clamped slab of reinforced concrete. As the Abaqus version 6.10-1 did not have the HJC model in its library, it was used the JH2 model, which is already available in this finite element software and a comparison of different penetrator geometries was made.

2. Modelling Strategy

The penetration bomb was assumed to be made of two different materials: a metallic case, which was modeled with a Johnson Cook model, and an explosive payload, which was modeled with an Equation of State (EOS).

To compare the effect of the ogive geometry on the impact process, it was mounted three different geometries with the same diameter, and the same mass to have the equivalent kinetic energy in all cases. The chosen geometries of the ogives were hemispherical, conical with 400 and conical with 600. The mass was adjusted modifying the length of the explosive, keeping the shell thickness equals to 1 inch, and the diameter of the top of the truncated cone equals to 0.3 m for all geometries.

The geometries of the penetration bombs studied are depicted in figure 1:

Vol.2 Issue.4,
April 2014.
Pgs: 38-52

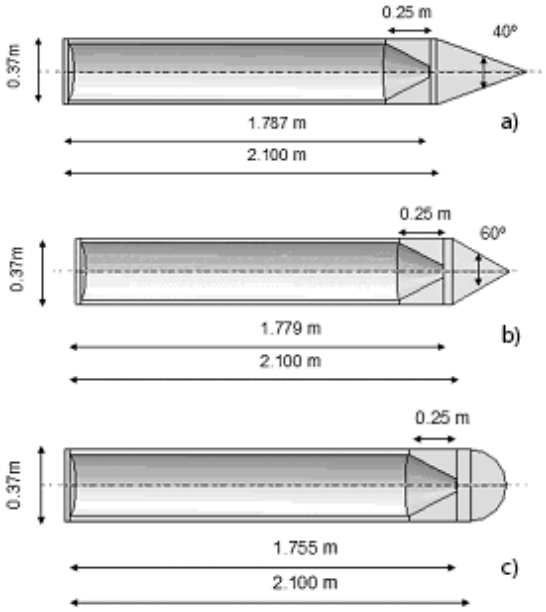

Figure 1: a) Geometry of the first conical ogive with an angle of 400, b) Geometry of the second conical ogive with an angle of 600, c) Geometry of hemispherical ogive.

2.1 Case modeling

The case of the bomb is made of high strength steel such as the AISI 4340. To perform the modeling, it was used the Johnson Cook model for metals (1983). The effect of the change in temperature during the penetration process was not included in the model. The Von Mises equivalent stress, disregarding the temperature effects, is given by eq. (1):

$$\sigma = \left(A + B\varepsilon^{n}\right)\left(1 + C\ln\dot{\varepsilon}^{*}\right) \tag{1}$$

where ε is the equivalent plastic strain, $\dot{\varepsilon}^{*} = \dot{\varepsilon}/\dot{\varepsilon}_{0}$ is the dimensionless equivalent strain rate (for reference, $\dot{\varepsilon}_{0}$ = *1/s*). The four constants of this model are: A, B, n and C. To model the metal failure it was used the Johnson Cook failure model (Johnson and Cook, 1983). In this model, the failure plastic strain is given by eq. (2):

$$\varepsilon_{p}^{f} = \left(D_{1} + D_{2}\exp D_{3}\sigma^{*}\right)\left(1 + D_{4}\ln\dot{\varepsilon}^{*}\right) \tag{2}$$

The dimensionless stress is given by $\sigma^{*} = \sigma_{m}/\sigma$, where σ_{m} is the mean of the three principal stresses, and σ is the Von Mises stress given by eq. (1). As the values of σ and ε are not constants, it is necessary to calculate the damage variable in each integration step. The damage variable D is defined by eq. (3) and the element is assumed to be fully failed when (D = 1).

$$D = \sum \frac{\Delta\varepsilon^{p}}{\varepsilon_{f}^{\,p}} \tag{3}$$

$\Delta\varepsilon^p$ is the accumulated plastic strain in one integration cycle, and $\varepsilon_f{}^p$ is the plastic strain at failure given by eq. (2).

2.2 Explosive Modeling

A pure hydrostatic behavior defined in terms of a polynomial Equation of State (EOS) proposed by Schwer and Day (1991) was assigned to the explosive. The EOS for the explosive is given by eq. (4).

$$P = C_0 + C_1\mu + C_2\mu^2 \tag{4}$$

where C_0, C_1 and C_2 are constants, C_1 is the bulk modulus, $\mu = (\rho/\rho_0) - 1$, ρ is the instantaneous density, and ρ_0 is the initial density. The values $C_0 = C_2 = 0$, C_1 =68.9 kbar and $\rho_0 = 1.75 g/cm^3$ where taken from Schwer and Day (1991). This equation of State is not available in Abaqus Explicit and was implemented within brick elements as an user-defined material model (VUMAT).

2.3 Target Modeling

The shelter was assumed to be made of reinforced concrete with dimensions of 4,0 m x 4,0 m x 1,5 m, as shown on fig. 4. The steel reinforcement was placed inside the concrete, modeled with nonlinear beam elements with elastoplastic constitutive model. To model the concrete was used solid hexahedron elements. To connect the concrete to the steel reinforcement, it was used the Abaqus command *EMBEDDED ELEMENT which searches for the geometric relationships between nodes of the embedded elements and the host elements. If a node of an embedded element lies within a host element, the translational degrees of freedom at the node are eliminated and the node becomes an "embedded node." The translational degrees of freedom of the embedded node are constrained to the interpolated values of the corresponding degrees of freedom of the host element (Abaqus Theory Manual, 2010). It was used 6 layers of steel reinforcement, distanced 150 mm each, 50 mm of the boundaries and 800 mm on the central layers, as shown on fig. 2.

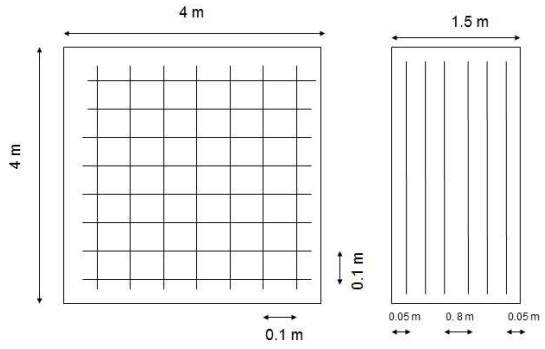

Figure 2: Target geometry with location of the steel reinforcement (12.5 mm diameter).

To model the concrete, it was chosen the JH2 (Johnson and Holmquist, 1993) model which was adapted to simulate the behavior of brittle materials subjected to high strains, strain rates and pressure. The equivalent stress is a function of the static resistance, fracture strength, strain, strain rate, pressure and a damage variable (D). The

equivalent stress and the pressure are normalized by the Hugoniot Elastic Limit (HEL). The stress at HEL is defined by eq. (5):

$$\sigma_{HEL} = \frac{3}{2}(HEL - P_{HEL}) \tag{5}$$

Where the HEL is the one-dimensional Hugoniot Elastic Limit, and P_{HEL} is the pressure component at HEL. The equivalent Stress is given by eq. (6):

$$\sigma^* = \sigma_i^* - D(\sigma_i^* - \sigma_f^*) \tag{6}$$

Where the equivalent tension is normalized by the equivalent tension at HEL, eq. (7):

$$\sigma^* = \frac{\sigma}{\sigma_{HEL}} \tag{7}$$

The equivalent tension of the intact material is given by eq. (8):

$$\sigma_i^* = A(P+T)^n(1+C\ln\dot{\varepsilon}^*) \tag{8}$$

And the equivalent tension at failure is given by (9):

$$\sigma_f^* = B(P)^m(1+C\ln\dot{\varepsilon}^*) \tag{9}$$

The model constants are: A, B, C, m, n and $S_{\max}$. T is the maximum hydrostatic tensile stress supported by the material. The strain rate is given by $\dot{\varepsilon}^* = \dot{\varepsilon}/\dot{\varepsilon}_0$, with the reference value $\dot{\varepsilon}_0 = 1/s$. The damage evolution is very similar to Johnson Cook's model is given by eq. (10):

$$D = \sum \frac{\Delta\varepsilon^p}{\varepsilon_f^p} \tag{10}$$

where $\Delta\varepsilon^p$ is the plastic strain in one integration step, and $\varepsilon_f^p = f(P)$ is the plastic strain at failure, given by eq. (11):

$$\varepsilon_f^p = D_1(P^* + T^*)^{D_2} \tag{11}$$

D_1 and D_2, are the material constants. Usually, it is not possible to perform tests of specimens at high pressures of interest, thus, the damage functions and the fracture resistances have to be inferred by other means like impact tests. The hydrostatic behaviour is defined by a polynomial Equation of the State given by eq. (12),

$$P = K_1\mu + K_2\mu^2 + K_3\mu^3 \tag{12}$$

K_1, K_2 e K_3 are constants, K_1 is the bulk modulus, $\mu = (\rho/\rho_0) - 1$, where ρ is the instantaneous density, and ρ_0 is the initial density. For tensile stresses, the eq. (12) is modified to $P = K_1\mu$.

When damage ($D > 0$), there is a pressure increment ΔP, determined by energy methods, then, we have the eq. (13):

$$P = K_1\mu + K_2\mu^2 + K_3\mu^3 + \Delta P \tag{13}$$

The pressure increment is determined from energy considerations: it varies from $\Delta P=0$ at $D=0$ to $\Delta P=\Delta P_{max}$ at $D=1$. The incremental internal elastic energy decrease due to shear and deviator stress is converted to potential internal energy by incrementally increasing ΔP. The decrease in the shear and deviator stress occurs because the strength decreases as damage increases .The expression for the elastic internal energy of shear and deviatoric stress is given as follows,

$$U = \frac{\left(\sigma_{HEL}\sigma^*\right)^2}{6G} \tag{14}$$

where G is the shear modulus of elasticity. The incremental energy loss is given by

$$\Delta U = U_D^t - U_D^{t+\Delta t} \tag{15}$$

where U_D^t and $U_D^{t+\Delta t}$ are computed from Eq. 14 using the updated stresses at the current step $\sigma^{t+\Delta t}$ for both energies. Johnson and Homquist shown that if the energy loss ΔU is converted to potential hydrostatic energy through ΔP the following equation, for the pressure increment can obtained,

$$\Delta P^{t+\Delta t} = -K_1\mu^{t+\Delta t} + \sqrt{\left(K_1\mu^{t+\Delta t} + \Delta P^t\right)^2 + 2\beta K_1 \Delta U} \tag{16}$$

where β is the fraction of the elastic energy loss converted to potential hydrostatic energy. It is usual to find in the literature a model called HJC for concrete (Holmquist et al., 1993) which has a mathematical formulation very similar to the JH2. The expression for the undamaged equivalent stress, given by the HJC model, is shown on eq. (17):

$$\sigma_i^* = \left(A(1-D) + BP^{*n}\right)(1 + C\ln\dot{\varepsilon}^*) \tag{17}$$

The stress is normalized by f_c, which denotes the quasi-static strength for unconfined concrete. Then, the normalized equivalent tension is given by $\sigma^* = \sigma / f_c$, where σ is the equivalent stress. P^* is the normalized pressure given by $P^* = P/f_c$. The strain rate is given by $\dot{\varepsilon}^* = \dot{\varepsilon}/\dot{\varepsilon}_0$, where $\dot{\varepsilon}$ denotes the current strain rate and $\dot{\varepsilon}_0 = 1/s$ is the reference strain rate. The damage parameter is given by D ($0 < D < 1$) and the normalized maximum tensile stress is $T^* = T/f_c$, where T is the maximum tensile stress.

The damage variable is given by eq. (18):

$$D = \sum \frac{\Delta\varepsilon^p + \Delta\mu^p}{\varepsilon_f{}^p + \mu^p} \tag{18}$$

The HJC damage model is very similar to the Johnson Cook and JH2, but it includes the term of plastic volumetric strain $\Delta\mu^p$. The factor $\Delta\varepsilon^p$ is the plastic strain accumulated in one the integration step. The failure strain is given by eq. (19):

$$\varepsilon_f{}^p + \mu^p = D_1(P^* + T^*)^{D_2} \tag{19}$$

where D_1 and D_2 are the material damage constants.

The equation of the state for HJC model is divided into 3 regions, being 2 linear and one polynomial. It is shown in (Abaqus Theory Manual, 2010) that the model JH2 can predict very accurately the penetration process in brittle materials subjected to high velocity impact. As the software used for the numerical simulation (Abaqus – v. 6.10-1) doesn't have the HJC model in its library, it was used the JH2 model with the same normalized parameters of HJC. To use the same normalization, it was used the values of $\sigma_{HEL} = f_c$ and $P_{HEL} = f_c$ in eq. (20):

$$\sigma_{HEL} = \frac{3}{2}(HEL - P_{HEL}) = f_c \tag{20}$$

Using the eq. (20) it is possible to determine the Hugoniot Elastic Limit (HEL). When *n=0*, the equations (6) and (17) become equal and the remaining differences between the HJC model and the JH2 model come from the Equation of the State (EOS) and the damage parameter, which includes the value of volumetric plastic strain, $\Delta\mu^p$, on the HJC model.

3. Numerical Simulations

3.1 Model validation

The results of Hanchack's experiments (Hanchack et al., 1992), which were performed in a impact speed range of 381 to 1058 m/s have been used to validate the model. Hanchack's reinforced concrete target had a 48 MPa unconfined tensile strength, with dimension of 610 x 610 x 178 mm3. In the interior of the concrete there were 3 layers of squared-pattern reinforcement made with 5.69 mm diameter steel wire. The constructive details of the target are given in (Hanchack et al., 1992). The projectile had length of 143.7 mm with diameter of 25.4 mm, and caliber-radius head (CRH) ratio of 3, as shown in Figure 4.

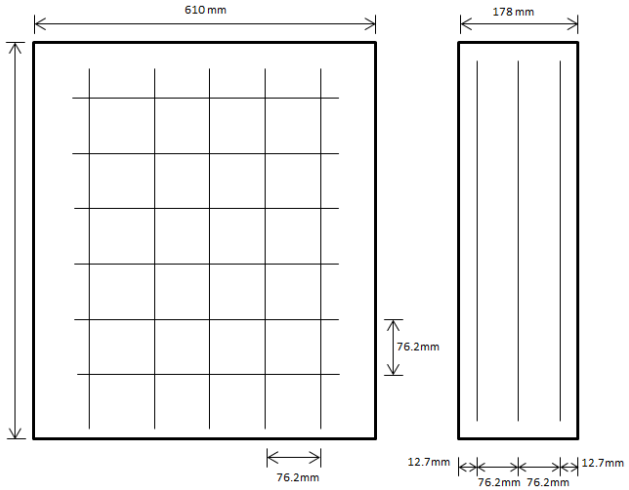

Figure 3: Target geometry with location of the steel reinforcement (5.69 mm diameter).

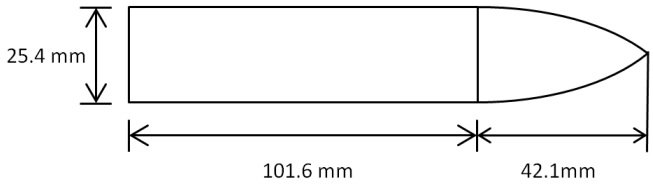

Figure 4: Projectile geometry (0.50 kg).

To simulate Hanchak´s experiment, it was used a 1/4 symmetric model, as shown in Figure 5. The material properties were taken from the open literature. Table 3 shows the material parameters used for the concrete. It was used eq. (20) to change the (Islam et al., 2011) HJC material parameters for concrete into JH2 parameters to use in Abaqus. It was used an elastoplastic model do simulate the projectile and the reinforcement. The constants were taken from Martin (2010) and (Hanchack et al., 1992), and showed in table 2 and 3 respectively.

Table 1: Material constants for the projectile

E (GPa)	*v*	*ρ(kg/m³)*	*Yield Strength (MPa)*	*Ultimate Strain*
206	0.3	8020	1700	0.15

Table 2: Material constants for the metallic reinforcement

E (GPa)	*v*	*ρ (kg/m³)*	*Yield Strength (MPa)*	*Ultimate Strain*
199	0.3	7850	220	0.15

Table 3: Material constants for a 48 MPa unconfined strength concrete

G (GPa)	*ρ (kg/m³)*	*A*	*n*	*B*
14.86	2440	0.79	0	1.6
m	*C*	$\dot{\varepsilon}_0$	$S_{\max}$	*T (MPa)*
0.61	0.007	1	7	3.54
$\varepsilon^f_{p\,\max}$	$\varepsilon^f_{p\,\min}$	K_1 *(GPa)*	K_2 *(GPa)*	K_3 *(GPa)*
1.0	0.01	85	-171	208
HEL (MPa)	P_{HEL} *(MPa)*	D_1	D_2	
80	48	0.004	1	

Vol.2 Issue.4,
April 2014.
Pgs: 38-52

The steel reinforcement of the concrete was placed inside the concrete, and modeled with bar elements, the concrete with hexahedron elements, and the projectile with tetrahedron elements. To connect the concrete to the steel reinforce, it was used the Abaqus command *EMBEDDED ELEMENTD described in section 2.3. The mesh used is finer in the region of the impact, because the damage was seen only in a region twice the size of the projectile diameter, as shown in Figure 6.

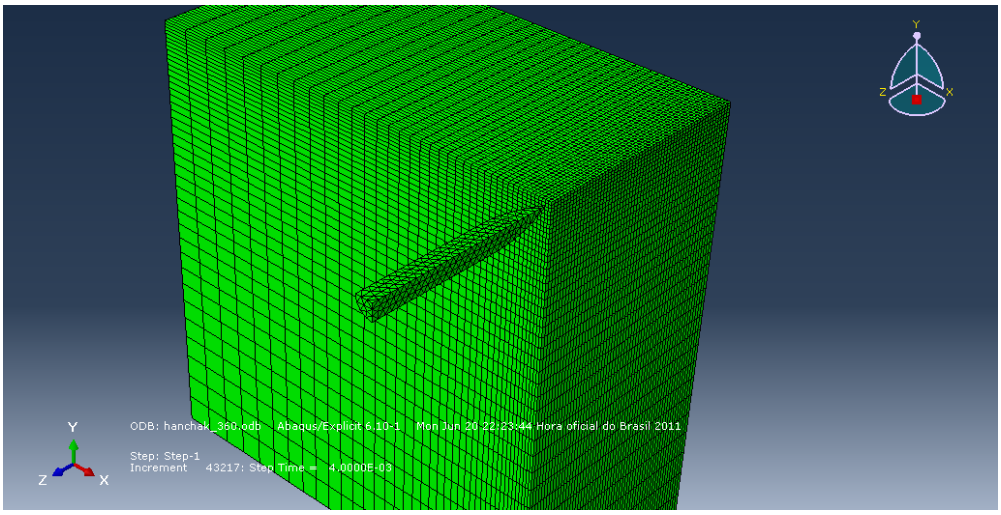

Figure 5: Finite Element Mesh used with ¼ symmetry.

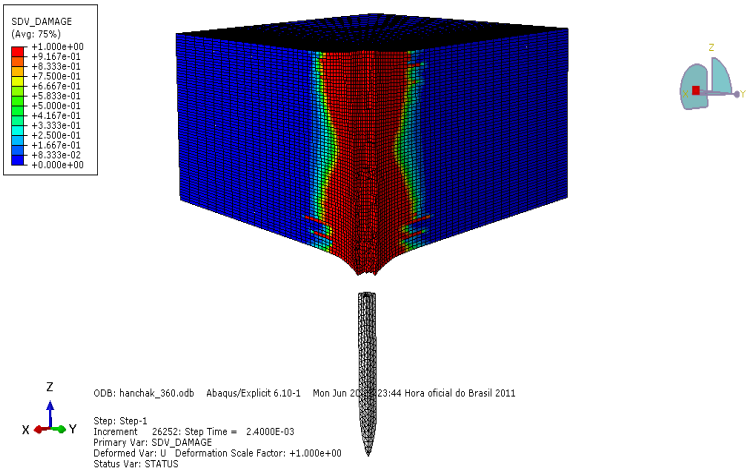

Figure 6: Damage fringe for impact velocity of 360 m/s.

A comparison between numerical and the experimental results are depicted in Figure 7. In a general way, a very good agreement was found between numerical and experimental results for the full-range of simulated impact velocity.

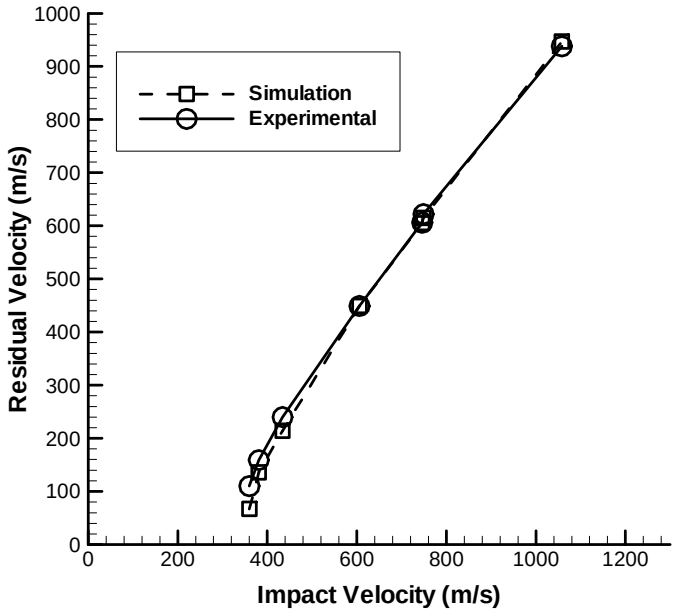

Figure 7: Comparison between numerical and experimental results taken from (Hanchak et al. ,1992).

3.2 Simulated impact scenarios for the penetration bomb

The simulations were carried out using the Abaqus Explicit FE code version 10.11-1. The proposed models account for damage prediction on the concrete slab and penetration bomb, during the penetration process. In the simulation, it was used a 1/2 symmetric model, as shown in Figure 8 to reduce the computational time by the same order of magnitude. It was studied 2 different impacts scenarios: one normal, and other with an impact angle of 5^0. Tables 2 to 4 show the material constants used in the simulations. The material constants for the metal case were taken from (Johnson and Cook, 1983) and (Johnson and Cook, 1985).

Table 4: Material constants for the metallic case made of AISI 4340 steel.

E (GPa)	ν	ρ (kg/m³)	C_1 (MPa)	C_2 (MPa)
211	0.3	7850	792	510
C_3	D_1	D_2	D_3	D_4
0.26	0.05	3.44	-2.12	0.002

The mesh used is finer in the impact region(Fig. 8) because the damage was seen only in a region 3 times the size of the bomb diameter (Fig. 9).

Vol.2 Issue.4,
April 2014.
Pgs: 38-52

The model considered in this work does not simulate the effect of the tail and the fuse structures on the dynamic of the impact. It can be added lumping masses on the model to simulate these structures with equivalent kinetic energies. Due to the fluid characteristic of the explosive, it is necessary to increase the bulk viscosity of the simulation from 0.06 to 0.4.

Figure 10 shows the predicted residual velocity for the three geometries studied in this, named conic_01 for the 400 ogive, conic_02 for the 600 ogive, and spherical for the semi hemispherical ogive. The incident impact angles assumed in this study were 00 and 50. The impact velocities were varied from 300 to 450 m/s for each impact scenario. The results indicate that for impact incident angles of 50, the residual velocity decreases when compared with impact incident angles of 00 (normal impact). This behavior is explained by the larger contact area between the projectile and the shelter which increases the friction effects between the bodies in contact decelerating even more the projectile velocity when compared to the normal impact scenario. Furthermore, for the impact incident angles different from 00 the target volume affected by the projectile is also more pronounced compared to normal impact cases which also corroborates with the projectile deceleration.

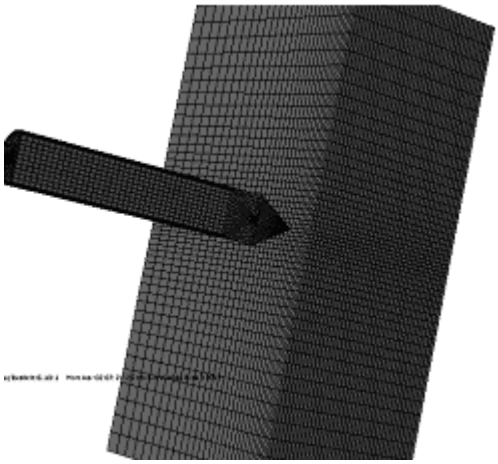

Figure 8: Model of the 600 ogive penetration bomb, with symmetry of 1/2.

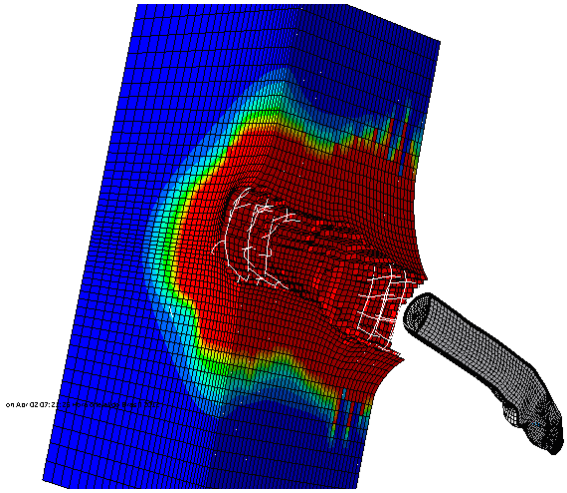

Figure 9: Fringe of damage variable D after the 50 and 450 m/s velocity impact of the 600 ogive.

Vol.2 Issue.4,
April 2014.
Pgs: 38-52

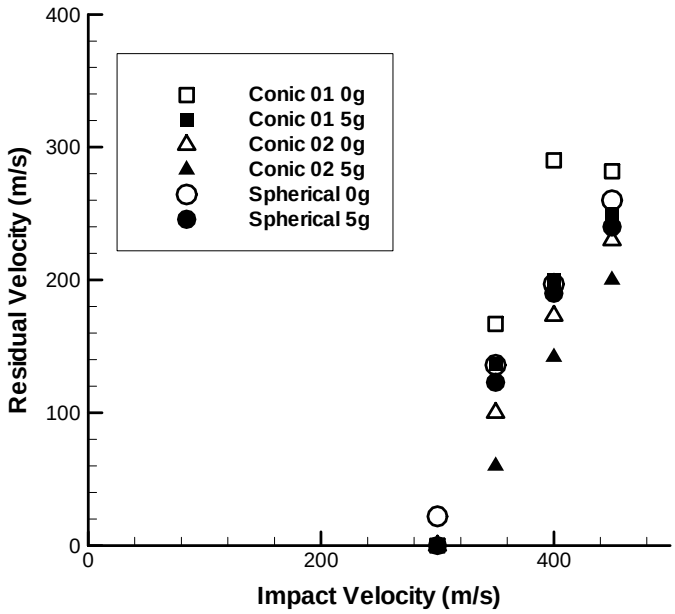

Figure 10: Residual velocity versus impact velocity for 3 ogives and 2 angles of impact.

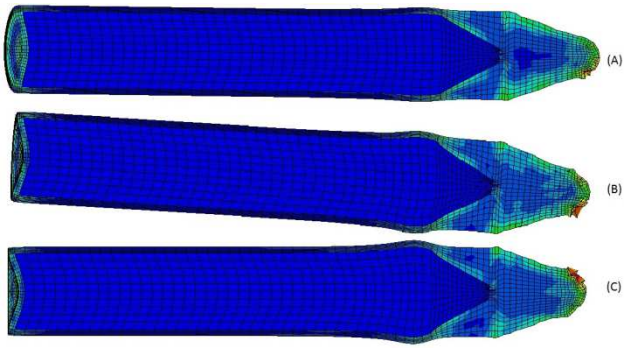

Figure 11: Final shape of the 400 ogive bomb, with impact velocities of (A) 350m/s, (B) 400m/s and (C) 450 m/s, and 00 impact angle.

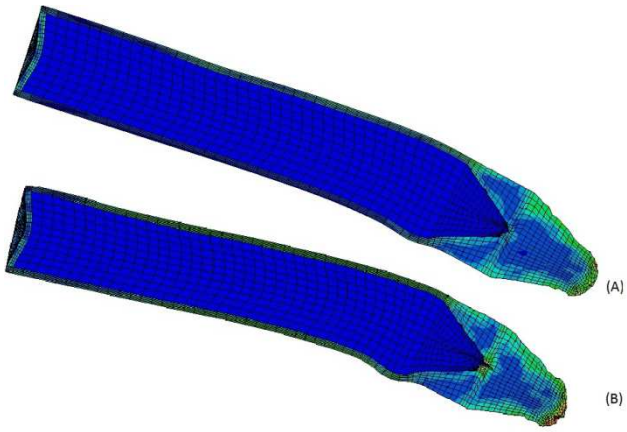

Figure 12: Final shape of the 400 ogive bomb, with impact velocities of (A) 350 m/s and (B) 400 m/s, and 50 impact angle.

Figs. 11 and 12 show that higher the impact velocity more pronounced is the deformation in the metallic case of the penetration bomb, as expected. The same behavior was obtained for all the three geometries studied in this work.

On fig. 10 it can be observed that for the impact velocity of 300 m/s, only the semi hemispherical ogive shape perforated the target. For velocities above 350 m/s the residual velocities of the 400 ogive shape are higher than the semi hemispherical ogive projectile. The simulations also indicate that increasing the impact velocity of the 400 ogive from 400 to 450 m/s implies in a reduction of the residual velocity . This behavior was observed only in this geometry, and one possible cause that may explain this behaviour is that part of the the kinetic energy is converted into deformation of the metal case.

The numerical results indicate that the 400 conical ogive projectile geometry exhibited a better ballistic performance compared to the 600 conical and semi hemispherical ogive shapes.

4. Conclusion

This work presented a numerical methodology to model the impact of a penetration bomb on a concrete shelter. The JH2 and the Johnson Cook constitutive models were used to simulate the concrete shelter and the bomb metallic case, respectively. A polynomial Equation of State was implemented into Abaqus to simulate the behavior of the explosive.

With this numerical tool it is possible to improve the design of penetration bombs, optimizing its characteristics, and observing if its case will fail in the penetration process. The numerical methodology allows one to define the constraints for the launching envelope of new weapons. With this kind of simulation it is also possible to predict the projectile deceleration during the penetration process. This information is very useful to the fuse developer.

An experimental full scale testing programme is underway at ITA/IAE to validate the proposed model and results presented herein.

References

Abaqus Theory Manual version 6.10-1.

Ben-Dor, G.; Dubinsky, A. and Elpwrin, T., (2005). Ballistic impact: recent advances in analytical modelling of plate penetration dynamics - A Review, Applied Mechanics Review 58:355-371.

Cargile, J.D.; O'Neil, F. and Needley, B.D, (2002). Very high strength concretes for use in blast and penetration resistant structures", AMPTIAC Quaterly 6(4): 61-66.

Chen, X.W. and Li, Q.M. Deep., (2002). Penetration of a non-deformable projectile with different geometrical characteristics, International Journal of Impact Engineering 27: 619-637.

Chen, X.W.; Fan, S.C.; Li, Q.M., (2004). Oblique and normal perforation of concrete targets by a rigid projectile, International Journal of Impact Engineering 30:617-637.

Conrad, M.M., (2011). Projectile penetration into reinforced concrete: analysis of interaction and its experimental verification", Journal of the Mechanical Behavior of Materials 16:35–44.

DancYgier, A. N. and Yahkelevsky, D.Z., (1996). High strength concrete response to hard projectile impact, International Journal of Impact Engineering 18:583-599.

Hanchak, S.J.; Forrestal, M.J.; Young, E. R. and Ehrgott, J.Q. , (1992). Perforation of concrete slabs with 48 MPa and 140 MPa unconfined compressive strength, International Journal of Impact Engineering 12:1-7.

Holmquist, T.J; Johnson, G.R and Cook, W.H., (1993). A computational constitutive model for concrete subjected to large strains, high strain rates, and high pressures". In: International Symposium on Ballistics, 14., 1993, Quebec City: National Defense Research Establishment, p. 591-600.

Hughes, G. H., (2004). Missile impact on reinforced concrete, Nuclear Engineering and design 77:23-35.

Islam, Md. J.; Liu, Z. and Swaddiwudhipong, S., (2011). Numerical study on concrete penetration/perforation under high velocity impact by ogive-nose projectile, Computers and Concrete, 8 (1): 111-123.

Johnson, G.R and Holmquist, T.J. ,(1992). A computational constitutive model for brittle materials subjected to large strains, high strain rates, and high pressures. In: Meyers, M. A.; Murr, L. E.; Staudhammer, K. P. (Ed.). New York: Marcel Decker Inc.;. p. 1075-1081.

Johnson, G.R and Holmquist, T.J., (1994). An improved computational constitutive model for brittle materials, American Institute of Physics, 12:981-984.

Johnson, G.R and Cook, W.H., (1983). A constitutive model and data for metals subjected to large strains, high strain rates and high temperatures". In: International Symposium on Ballistics, 7., 1983, p. 541 - 547.

Johnson, G.R and Cook, W.H., (1985) Fracture characteristics of three metals subjected to various strains, strain rates, temperatures and pressures, Engineering Fracture Mechanics 21:31-48, 1985.

Kennedy I.,(1976). A review of procedures for the analysis and design of concrete structures to resist missile impact effects, Nucl Eng Des 37: 183-203.

Li, Q.M. and Chen, X.W., (2003). Dimensionless formulae for penetration depth of concrete target impacted by a non-deformable projectile, International Journal of Impact Engineering 28: 93-116.

Liam, Y.P.; Zhang, X.; Zhou, X. and Ma, Z.T., (2011). A FEMP method and its application in modeling dynamic response of reinforced concrete subjected to impact loading. Journal of the Computational Methods in Applied Mechanics and Engineering 200:1659-1670.

Liu, Y.; Huang, F. and Ma, A.,(2011). Numerical simulation of oblique penetration into reinforced concrete targets, Computer and Mathematics with Applications 61:2168-2171.

Martin, O.,(2010). Comparison of different constitutive models for concrete in ABAQUS/Explicit for missile impact analyses, JRC Scientific and Technical Reports, Luxembourg.

Melo, T.B.N., (2011). "Modelagem Numérica de Impacto em Concreto Armado Utilizando o Método dos Elementos Finitos". 84f. MSc. Thesis (in portuguese) - Instituto Tecnológico de Aeronáutica, São José dos Campos.

Polanco-Loria, M.; Opperstad, O.S.; Borvik, T. and Berstad, T., (2008). Numerical predictions of ballistic limits for concrete slabs using a modified version of the HJC concrete Model, International Journal of Impact Engineering 35:290-303.

Rahman, I. A.; Zaidi, A. M. A. and Latif Q. B. I., (2010). Review on Empirical Studies of Local Impact Effects of Hard Missile on Concrete Structures, International Journal of Sustainable Construction Engineering and Technology 1(1): 193-212.

Riedel, W.; Thoma K.; Hiermaier and S. Schmolinske, E.,(1997). Penetration of reinforced concrete by BETA-B-500 : numerical analysis using a new macroscopic concrete model for hydrocodes, International Symposium on Interaction of the Effects of Munitions with Structures, Virginia-USA.

Schwer, L.E. and Day, J., (1991). Computational techniques for penetration of concrete and steel targets by oblique impact of deformable projectiles, Nuclear Engineering and Design 215: 215-238.

Svinsas, E.; O'Carol, C.; Wentzel, C. M. and Carlberg, A., (2011). Benchmark trial designed to provide validation data for modeling, International Symposium on Interaction of the Effects of Munitions with Structures, San Diego-CA.

Tai, Y.S., (2009). Flat ended projectile penetrating ultra high strength concrete plate target, Theoretical and Applied Fracture mechanics 51:117-128.

Tai, Y.S. and Tang, C.C., (2006). Numerical simulation: the dynamic behavior of reinforced concrete plates under normal impact, Theoretical and Applied Fracture mechanics 45:117-127.

Taylor, L. M.; Chen, E. P. and Kuszumaul, J. S., (1986). Microcrack-induced damage accumulation on brittle rock under dynamic loading, Journal of the Computational Methods in Applied Mechanics and Engineering 55:301–320.

Teng, T.L.; Chu, Y.A. and Chin, H.S.,(2004). Simulation model of impact on reinforced concrete, Cement and Concrete Research 34:2067-2077.

Unusson, M. and Nilsson, L., (2006). Projectile penetration and perforation of high performance concrete: experimental results and macroscopic modeling,. International Journal of Impact Engineering 32:1068-1085.